

Magnetic structure of vortex and antivortex states in patterned Co elements studied by using scanning ion microscopy with polarization analysis

Jian Li and Carl Rau^{a)}

Department of Physics and Astronomy, Rice Quantum Institute and Center for Nanoscience and Technology, Rice University, Houston, Texas 77251

(Presented on 2 November 2005; published online 18 April 2006)

Scanning ion microscopy with polarization analysis (SIMPA) is used to investigate the surface magnetic structure of patterned Co elements created *in situ* by focused ion-beam lithography from thin (30 nm) Co films deposited on Si(100) substrates by electron-beam evaporation. The diameter d of the circular-shaped Co elements is varied between 5 and 38 μm . Three-dimensional, spin- and spatially resolved SIMPA spin maps directly reveal the *nonuniform* micromagnetic structure of magnetic vortex and antivortex states. They are dominated by a circular or hyperbolic surface magnetization profile with a wide vortex or antivortex core in the center with a perpendicular surface magnetization component which decreases with increasing distance from the core. Varying d , the vortex wall thickness can be changed from 0.6 to 4.2 μm . For Co elements with $d < 13 \mu\text{m}$, only single magnetic vortex states are found, whereas for $d > 13\text{--}15 \mu\text{m}$, magnetic multivortex and antivortex states are observed. © 2006 American Institute of Physics.

[DOI: 10.1063/1.2165596]

Quite recently, studies of magnetic vortex and antivortex domain structures in patterned magnetic elements have received great attention, not only because of their theoretical and experimental interests in studying a wealth of fundamental magnetization structures, but also because of their pivotal importance for the development of highly sophisticated magnetic devices.

There are a series of very interesting studies on the existence, observation, movement, and annihilation of magnetic vortices.¹⁻⁹ Using magnetic force microscopy (MFM), Lorentz microscopy (LM), a combination of surface magneto-optical Kerr effect (SMOKE) hysteresis loops, off-axis holography in transmission electron microscopy, and scanning electron microscopy with polarization analysis (SEMPA), it was possible to indirectly or directly verify the presence of magnetic vortices in patterned magnetic elements.¹⁻⁶ In some of the experiments, it was shown that magnetic vortices possess predominantly an in-plane magnetization profile and a core with a perpendicular magnetization which has been found to dominate the nanosecond magnetization dynamics of NiFe elements.^{8,9}

There is presently no fundamental information available about the detailed *three-dimensional* (3D) spin structure of magnetic vortices which could help to obtain more insight into the physical properties of magnetic vortices.

The 30-nm-thick polycrystalline Co films are evaporated on Si(100) substrates.¹⁰ The Co/Si(100) samples are inserted in a UHV chamber, where SMOKE hysteresis loops are recorded. From all samples, perfectly square magnetic hysteresis loops with a low coercivity field $H_c = 1178 \text{ A/m}$ (14.8 Oe) are found.¹¹ No changes size and shape of the square loops are observed upon rotation of the sample

around the surface normal due to the very good polycrystalline nature of the Co films.^{12,13} Therefore, these films should possess a very small reduced anisotropy constant Q given by $Q = K_r/K_d$, where K_r is an appropriate residual anisotropy coefficient and K_d is the stray field energy coefficient. For $K_r = H_c M_s / 2\mu_0$, $K_d = M_s^2 / 2\mu_0$, and $M_s = 1.4 \times 10^6 \text{ A/m}$, we obtain $Q = H_c / M_s = 8.4 \times 10^{-4}$.

Subsequently, the samples are transferred *in situ* from the SMOKE chamber to the SIMPA microscope, which is operated in the low 10^{-10} Torr region. In SIMPA, a micro-focused (spot size: 35 nm) 25 keV Ga^+ ion beam is scanned across a magnetic/nonmagnetic surface causing the emission of spin-polarized/non-spin-polarized electrons.^{11,14} The electrons emitted from the sample surface are collected by using an extracting lens system, and the electron-spin polarization (ESP) is measured using a Mott polarimeter. The magnitude and orientation of the spin polarization P vector of the ion-induced emitted electrons is directly proportional to the magnitude and orientation of the surface magnetization (SM) vector of the local surface area probed by the focused ion beam.^{11,14,15} P is defined by $P = (n^+ - n^-) / (n^+ + n^-)$, where n^- and n^+ represent the density of electrons with spin moment parallel and antiparallel, respectively, to the SM vector.¹⁶ The inelastic mean-free path of the emitted electrons amounts to only a few monolayers,¹⁷ which explains the high surface sensitivity of SIMPA. We note that SIMPA does not modify micromagnetic configurations during the measurements which is found from subsequently taken SIMPA images.¹⁸ In previous SIMPA experiments, the two in-plane components of P were studied and C , S , and cross-tie magnetization distributions could be directly identified.^{11,15} Here, we are detecting all 3D components of the ESP P of the emitted electrons. For details, we refer to Refs. 11, 14, and 15.

^{a)}Electronic mail: rau@rice.edu

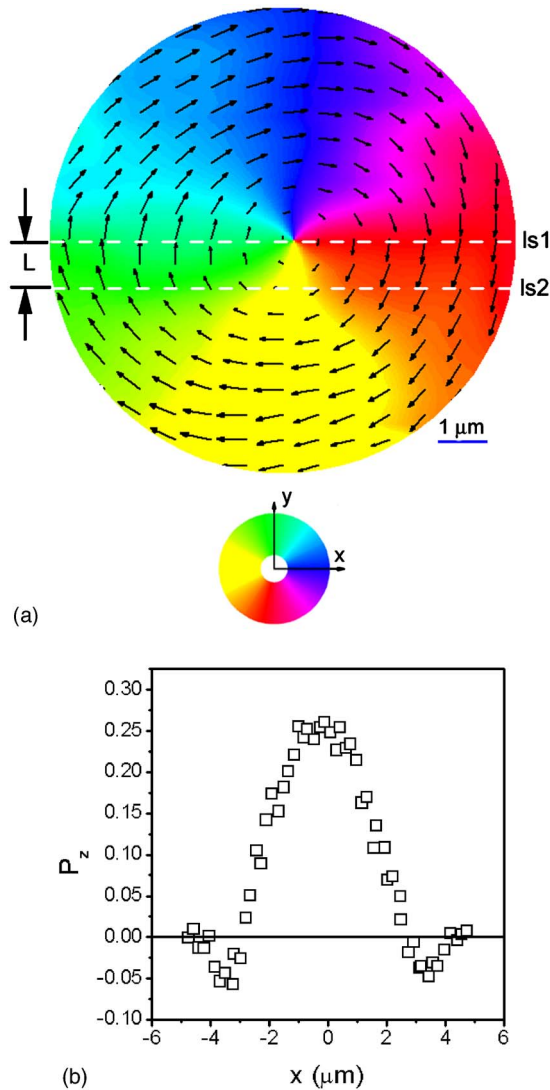


FIG. 1. (Color online) (a) SIMPA spin map obtained at the surface of a $d=9.5\ \mu\text{m}$ Co disk. The gray shades represent different orientations of the in-plane polarization P as given by the gray shade wheel shown in the lower part of (a) together with the x and y axes. The z axis is defined as $x \times y$. The local orientation and magnitude of the P vectors is given by black arrows, the magnitude of P being proportional to the length of the arrows. In order to obtain a clear plot of the P vectors (maximum value 25%) and to account for statistical fluctuations in count rates, P is averaged over four nearest-neighbor points and then only every fourth P vector is plotted, thereby reducing the density of P vectors by a factor of 64. Two white-dashed lines ls1 ($y=0$) and ls2 ($y=-L$) represent SIMPA line scans [for details, see Figs. 1(b) and 2(a)]; (b) ESP results for the perpendicular polarization component P_z along the line ls1.

Circular-shaped Co disks of sizes between 5 and $38\ \mu\text{m}$ are fabricated by using focused ion-beam (FIB) etching. The magnetic structure can immediately be studied *in situ* by using SIMPA. For SIMPA imaging, ion currents of about 80 pA are used, whereas for ion-beam milling, currents of about 1 nA are utilized.

Figure 1(a) shows a spin- and spatially resolved SIMPA spin map obtained at the surface of a FIB-created, circular (diameter $d=9.5\ \mu\text{m}$) Co (30 nm thick)/Si(100) element. From the distribution of the P vectors, it is clearly visible that the SM is *nonuniform* (noncollinear) and exhibits predominantly circular in-plane components. Due to the negli-

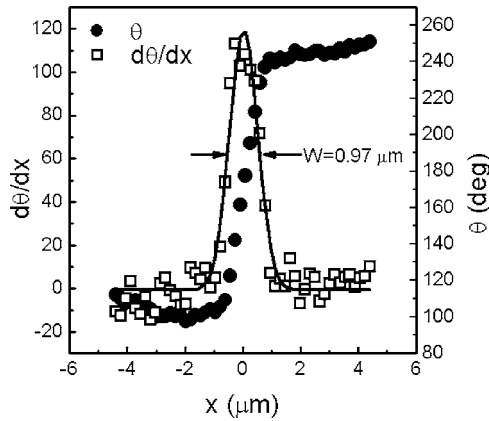
gible magnetocrystalline anisotropy ($Q=8.4 \times 10^{-4}$) of the elements, as expected, no domains with *uniform* SM are found. The distribution of the P vectors directly shows the existence of a single vortex with a curling vortex wall structure. From Fig. 1(a), there is a possible indication that the magnitude of the in-plane ESP decreases with decreasing distance to the center of the vortex, where it becomes zero implying the existence of nonzero, perpendicular SM components. For the measurement of P_z , a second SIMPA image is taken with the sample rotated 45° around the y axis. P_z is obtained from $P_x^{45}=(P_x-P_z)0.707$, with P_x being the measured x component of the ESP before rotating and P_x^{45} the x component of the ESP measured at 45° .^{11,19}

Figure 1(b) shows the results of a horizontal SIMPA line scan [see white-dashed line ls1 in Fig. 1(a)] of P_z through the center of the vortex. At the center of the vortex, P_z exhibits a maximum value (25%) and decreases, with increasing distance from the center of the vortex. These findings verify the existence of a vortex with a wide core ($|x| < 2.8\ \mu\text{m}$) and an outer region ($2.8\ \mu\text{m} < |x| < 4.75\ \mu\text{m}$) where P_z changes similar to Friedel-like oscillations and becomes zero. Note that the reversed ESP in the outer region compensates partially the positive ESP in the core.²⁰

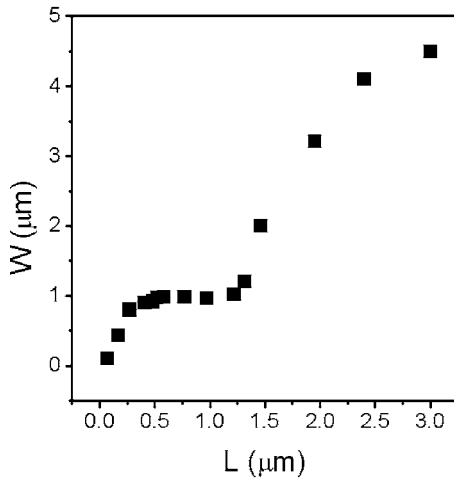
We note that from Fig. 1(a), at first sight, one cannot directly point to the existence of a vortex with a widely extended out-of-plane component of P . At $|x| \approx 2\ \mu\text{m}$, P_z amounts to 12.5% [see Fig. 1(b)], which amounts to 50% of the maximum P_z (25%) value. Using the maximum measured P value of 25%,¹¹ P_{\parallel} yields at $|x| \approx 2\ \mu\text{m}$ a value of 21.6% by using $P^2=P_{\parallel}^2+P_z^2$, which is hard to distinguish from 25% by using the graphical plot shown in Fig. 1(a). The origin of the existence of such a wide vortex, which is quite remarkable, might not only come from the very small Q value, but also from size effects. At first sight, the results of this paper for the vortex core width (approximately 50% of the total diameter) seem to be in contradiction with the results shown in Fig. 2 of Ref. 1. Unfortunately, in this paper no numeral values for the vortex core width could be obtained from MFM measurements, however, from their micro-magnetic simulations given in Fig. 1(b), one can derive a vortex core width of 20% of the total diameter of the vortex. We note that from the MFM images (Fig. 4 in Ref. 21) of circular CoCr dots of García-Martin *et al.*, one can derive vortex core widths of about 30%–40% of the total diameter of the vortices.²¹

We evaluate the domain-wall width W based on a classical definition, where the slope of the in-plane magnetization angle θ is used.²⁰ We use for W the half-width of the distribution of $d\theta/dx$ values as function of the x coordinate.

Figure 2(a) gives θ and $d\theta/dx$ as function of x for a horizontal SIMPA line scan across the line ls2 [see white-dashed line ls2 in Fig. 1(a)]. From this, we find for W a value of $0.97\ \mu\text{m}$ for L [see Fig. 1(a)] = $1\ \mu\text{m}$ and $d=9.5\ \mu\text{m}$. In Fig. 2(b), W is given as function of the distance L from the center of the $9.5\ \mu\text{m}$ diameter Co disk. From Fig. 2(b), we find that W exhibits a small value of 80 nm for $L=0.2\ \mu\text{m}$ and then rises to about $1\ \mu\text{m}$ at $L=0.4\ \mu\text{m}$, where it reaches a plateau and remains constant until $L=1.25\ \mu\text{m}$ and then increases slowly towards $4.5\ \mu\text{m}$ for $L=3\ \mu\text{m}$. It is obvious



(a)



(b)

FIG. 2. (a) SIMPA line scan for the in-plane magnetization angle θ and the slope $d\theta/dx$ along line ls2 [see Fig. 1(a)] as function of the x coordinate. The domain-wall width W is defined as the half-width of the Gaussian fitting curve (solid line) for the $d\theta/dx$ distribution; (b) domain-wall width W as function of L [see Fig. 1(a)].

that this dramatic change of W as function of L is caused by the interaction between exchange, magnetostatic, and anisotropy terms which depend strongly on L .

In subsequent SIMPA experiments, d is varied between 5 and 38 μm and W is evaluated as before for the 9.5 μm Co disk. From the results of these experiments, it is found that for each Co disk with diameter d , $W(L)$ exhibits a characteristic plateau as before for $d=9.5 \mu\text{m}$. We define this W value as a characteristic domain-wall thickness $W_{\text{ch}}(d)$. In Fig. 3, W_{ch} is shown as function of d . For $d=5 \mu\text{m}$, W_{ch} amounts to 0.6 μm and increases slowly with increasing d . Between $d=13\text{--}15 \mu\text{m}$, a sharp increase of W_{ch} is found. For $d > 16 \mu\text{m}$, W_{ch} amounts to 4.2 μm and remains nearly constant. We note, that from SIMPA spin maps, it is found that single vortex states exist only for $d < 13 \mu\text{m}$. For $d > 13\text{--}15 \mu\text{m}$, multivortex states consisting of single vortex and antivortex states with hyperbolical SM's are found. We believe that the findings shown in Figs. 2(b) and 3 provide valuable information for improving micromagnetic ground-state calculations for vortex states including domain-wall widths in patterned, soft magnetic materials.

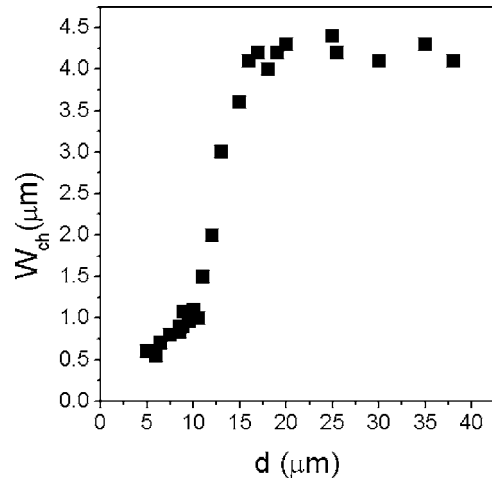


FIG. 3. Characteristic domain-wall width W_{ch} as function of diameter d of the Co disks.

For circular-shaped, polycrystalline, patterned Co elements with negligible magnetocrystalline anisotropy, the micromagnetic states consist, depending on the diameter of the elements, of magnetic vortex/antivortex states which possess a circular/hyperbolic SM profile with a central vortex/antivortex core with near completely perpendicular SM which decreases in the outer region similar to Friedel-like oscillations and becomes zero. It is found that, varying d , W_{ch} can be changed from 0.6 to 4.2 μm . The results show that SIMPA spin mapping can develop into an important and efficient tool to find desired, optimized micromagnetic states for patterned magnetic systems.

- ¹T. Shinjo, T. Okuno, R. Hassdorf, K. Shigeto, and T. Ono, *Science* **289**, 930 (2000).
- ²J. Raabe, R. Pulwey, R. Sattler, T. Schweinböck, J. Zweck, and D. Weiss, *J. Appl. Phys.* **88**, 4437 (2000).
- ³M. Schneider, H. Hoffmann, and J. Zweck, *Appl. Phys. Lett.* **77**, 2909 (2000); **79**, 3113 (2001).
- ⁴R. P. Cowburn, D. K. Koltsov, A. O. Adeyeye, M. E. Welland, and D. M. Tricker, *Phys. Rev. Lett.* **83**, 1042 (1999).
- ⁵R. E. Dunin-Borkowski, M. R. McCartney, B. Kardynal, D. J. Smith, and M. R. Scheinfein, *Appl. Phys. Lett.* **75**, 2641 (1999).
- ⁶A. F. Vaz *et al.*, *Phys. Rev. B* **67**, 140405 (2003).
- ⁷A. J. Freeman, K. Nakamura, and T. Ito, *J. Magn. Magn. Mater.* **272**, 1122 (2004).
- ⁸S. B. Choe *et al.*, *Science* **304**, 420 (2004).
- ⁹V. Novosad *et al.*, *Phys. Rev. B* **72**, 024455 (2005).
- ¹⁰W. C. Uhlig, H. Li, B. S. Han, and J. Shi, *J. Appl. Phys.* **91**, 6943 (2002).
- ¹¹J. Li and C. Rau, *J. Appl. Phys.* **95**, 6527 (2004).
- ¹²A. Fernandez, M. R. Gibbons, M. A. Wall, and C. J. Cerjan, *J. Magn. Magn. Mater.* **190**, 71 (1998).
- ¹³Y. Wu, J. Tsay, Sh. Chen, T. Fu, and Ch. Shern, *Jpn. J. Appl. Phys., Part 1* **40**, 6825 (2001).
- ¹⁴N. J. Zheng and C. Rau, *Mater. Res. Soc. Symp. Proc.* **313**, 723 (1993).
- ¹⁵J. Li and C. Rau, *J. Magn. Magn. Mater.* **286**, 473 (2005).
- ¹⁶C. Rau, *J. Magn. Magn. Mater.* **30**, 141 (1982).
- ¹⁷D. L. Abraham and H. Hopster, *Phys. Rev. Lett.* **58**, 1352 (1987).
- ¹⁸J. Li and C. Rau, *Nucl. Instrum. Methods Phys. Res. B* **230**, 518 (2005).
- ¹⁹M. Hoesch *et al.*, *J. Electron Spectrosc. Relat. Phenom.* **124**, 263 (2002).
- ²⁰A. Hubert and R. Schäfer, *Magnetic Domains: The Analysis of Magnetic Microstructures* (Springer-Verlag, Berlin, 1998).
- ²¹J. M. García-Martín, A. Thiaville, J. Miltat, T. Okuno, L. Vila, and I. Piraux, *J. Phys. D* **37**, 965 (2004).